Eur. Phys. J. B **5**, 163–168 (1998)

THE EUROPEAN PHYSICAL JOURNAL B

Investigations on the soft-mode mechanism of the ferroelectric phase transition in K_2ZnI_4

M. Jochum[a] and H.-G. Unruh

Fachrichtung 10.2 Experimentalphysik, Universität des Saarlandes, 66041 Saarbrücken, Germany

Received: 7 April 1998 / Revised: 5 June 1998 / Accepted: 16 June 1998

Abstract. Dielectric and Raman spectroscopic measurements have been performed to investigate the ferroelectric phase transition in K_2ZnI_4. Single crystals were grown by the zone melting method. The frequency dependence of the dielectric permittivity from 1 MHz to 1 GHz has been studied in a temperature range between 265 and 285 K. A Debye like dielectric dispersion was found, showing a critical slowing down around $T_c \approx 272$ K. Polarized Raman spectra have been taken between 220 and 310 K. Two softening modes have been found, one of A- and another one of B/B_g-symmetry. The phase transition mechanism in K_2ZnI_4 can be classified as partially order-disorder and partially displacive, confirming former structural results. It resembles strongly that of monoclinic K_2ZnBr_4.

PACS. 77.80.Bh Phase transitions and Curie point – 77.22.Gm Dielectric loss and relaxation – 78.30.-j Infrared and Raman spectra

1 Introduction

Among crystals with A_2BX_4-type formulae, there is a class of compounds which crystallize at ambient temperature in the Sr_2GeS_4-type structure [1] (monoclinic space group $P2_1/m$, $Z = 2$). Since the discovery of ferroelectricity in Tl_2ZnI_4 below 209 K by Gesi in 1985 [2], a growing number of halide compounds (X = Br, I) have been investigated and described in the literature (for an overview see [3]). So far the existence of a ferroelectric low temperature phase has been proved in K_2ZnBr_4 (α-modification) as well as in compounds with A = K, Tl, B = Co, Zn, X = I [4]. In all these substances, the spontaneous polarization appears along the monoclinic b-axis. In X-ray investigations on K_2ZnBr_4 [5–7] and K_2ZnI_4 [8] the space group of the ferroelectric phase was determined to $P2_1$, $Z = 2$; this space group is also assumed for all other ferroelectric compounds mentioned above.

Recently extensive X-ray and dielectric [7] as well as Raman spectroscopic [9] investigations provided a detailed picture of the transition mechanism in monoclinic K_2ZnBr_4. As a result, the transition in this compound was found to be driven by both ordering as well as displacive contributions. The order-disorder component could be verified by dielectric measurements in the microwave regime as a Debye like dispersion with a critical slowing down behaviour around T_c. A soft-mode of symmetry class A, found by Raman measurements, refers to the displacive contribution. This surprisingly complex behaviour as well as the relatively simple crystal structure make Sr_2GeS_4-type crystals an interesting new model-system for ferroelectric phase transitions.

In this paper we report on dielectric and Raman investigations on K_2ZnI_4. The crystal undergoes a ferroelectric phase transition at 272 K [10]. Kasano *et al.* [8] already solved the structure for both phases. The structure of K_2ZnI_4 as well as the displacement patterns from paraelectric to ferroelectric regime appear to be very similar to those of K_2ZnBr_4. Furthermore, Kasano *et al.* described the paraelectric structure to be partially disordered with respect to the ZnI_4^{2-}-tetrahedra, in analogy to their work on K_2ZnBr_4 [5]. Based on these results, we assumed that the K_2ZnBr_4 soft-mode model may also hold for K_2ZnI_4. Our results strongly support this assumption.

2 Crystal growth and preparation

Single crystals of K_2ZnI_4 were grown by the zone melting technique, using a slightly modified Bridgman furnace. A stoichiometric mixture of KI (99%, Fluka) and ZnI_2 (98.5%, Merck) was filled into a cylindrical glass capsule. Since both reagents are hygroscopic, the mixture was heated to about 150 °C in vacuum for several hours, then the capsule was sealed. The content of the capsule was cleaned up to 10 times by zone refining in the Bridgman furnace. Finally the single crystal was grown by pulling the capsule with a speed of 1.4 cm/d. The temperature gradient at the melt boundary was estimated to 5−10 K/cm. The obtained crystals (size: diameter 20 mm, height 20−50 mm) were clear, colorless and exhibit strong deliquescence. They decompose when coming into contact

[a] e-mail: mijoc@stud.uni-sb.de

with one of the usual solvents and even paraffin oil. So the crystals had to be stored in vacuum or in pure silicon oil. All preparations were made in a dry hot air stream or in a helium atmosphere. The relative humidity must be significantly less than 30%.

In order to orient the specimens, we used the fact that K_2ZnI_4 has a clear cleavage parallel to the a-plane [10], which can be found easily. The monoclinic axis lies parallel to a principal axis of the indicatrix and coincides therefore with one of the two extinction directions of a (100)-plate. It was clearly identified by means of polarization microscopy and low frequency dielectric measurements. In all three crystals we grew, the b-axis was not oriented parallel to the growth direction, as it was reported by Shimizu *et al.* [10]. Since we have no knowledge of the details of their crystal growth procedure, *e.g.* the shape of the capsule, we cannot make suggestions for the explanation of this deviation at present.

3 Dielectric measurements

Measurements of the dielectric dispersion along the monoclinic b-axis in the frequency range between 1 MHz and 1 GHz were performed by means of a coaxial reflectometer set-up. The cylindrical sample with its symmetry axis parallel to the crystallographic b direction is positioned in the center of a radial transmission line which forms the termination of a coaxial line [11]. The complex dielectric constant $\epsilon^* = \epsilon' - i\epsilon''$ is calculated from the reflection coefficient which is measured by one of two complex network analysers (HP4191 and HP8510B) depending on the frequency.

Owing to their strong deliquescence, K_2ZnI_4 crystals tend to build up a surface layer of hydrated material when coming into contact with humid air. Such layers can distort the bulk signal in dielectric measurements and may cause an additional and irreproducible dielectric dispersion. In analogy with the results of K_2ZnBr_4 [7], the high frequency dielectric response of K_2ZnI_4 is only reproducible for well prepared samples with ϵ_{max} significantly more than 1000. Therefore, we assume that only such samples exhibit an unaltered signal from the bulk. Merely such results are considered here.

Dispersion curves were measured in a temperature range between 265 K and 285 K. For each temperature, 90 frequencies were applied. The frequency points were chosen equidistantly on a logarithmic scale. Cole-Cole plots of the dielectric dispersion of a good sample are displayed in Figure 1 for the paraelectric and ferroelectric regime, respectively. The measurements have been evaluated by complex least-squares fits to the generalized Cole-Cole formula:

$$\epsilon^*(f) = \epsilon_h + \sum_{j=1}^{n} \frac{\Delta\epsilon_j}{1 + (i\ f/f_j)^{1-h_j}} \cdot \qquad (1)$$

Above T_c, $n = 1$ was adequate to describe $\epsilon^*(f)$. The distribution parameter h_1 is less than 0.02 within the investigated temperature range and reaches 0.006 around T_c.

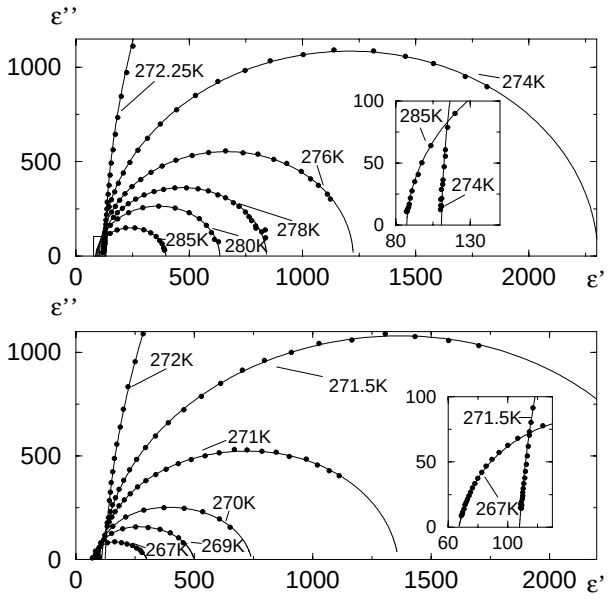

Fig. 1. The dielectric dispersion of K_2ZnI_4 at different temperatures. Above: paraelectric regime, below: ferroelectric regime. A detailed picture of the high frequency limits is displayed in the insets. The lines are fits according to (1).

Therefore the relaxation may be described as Debye like. Below T_c, a single Cole-Cole relaxator is insufficient to fit the experimental data satisfactorily. An additional Cole-Cole term (*i.e.* $n = 2$), however, gives good agreement with the measured $\epsilon^*(f)$ within the investigated temperature range. A comparison of the distribution parameters h_j, $j = 1, 2$ shows that the process with the higher characteristic frequency f_j coincides with the one in the paraelectric regime. This relaxation will be indexed as $j = 1$ henceforth.

The low frequency limits of the dielectric permittivity, $\epsilon_s = \epsilon_h + \sum_{i=1}^{n} \Delta\epsilon_i$, and $\epsilon_{s2} = \epsilon_h + \Delta\epsilon_1$, exhibit a Curie-Weiss behaviour within the observed temperature range (Fig. 2). ϵ_{s2} represents the contributions to ϵ^*, which occur in both phases. The temperature dependence of ϵ_s^{-1} above T_c is well-described by the formula

$$\epsilon_s^{-1} = \frac{T - T_0}{C} - \frac{\epsilon_\infty}{C^2} \cdot (T - T_0)^2 \qquad (2)$$

which approximates the classical Curie-Weiss law, if $\epsilon_\infty(T - T_0) \ll C$. This condition is fulfilled within the considered temperature range. We obtained $C \approx 5200$ K and $T_0 \approx 271.7$ K. ϵ_∞ ranged between 4 and 6. This value is relatively unprecise since the observed temperature range is too small to determine the noncritical part of the permittivity with a higher accuracy. However, it is certain that ϵ_∞ does not coincide with the high frequency limit of the permittivity, ϵ_h. Moreover, ϵ_h also shows a distinct temperature dependence and reaches a maximum of 128 at T_c (Fig. 2, diamonds). In order to account for the step in the permittivity from ϵ_∞ to ϵ_h, a second dispersion must exist at frequencies significantly higher than 1 GHz. This point will be discussed later in connection with the results of Section 4.

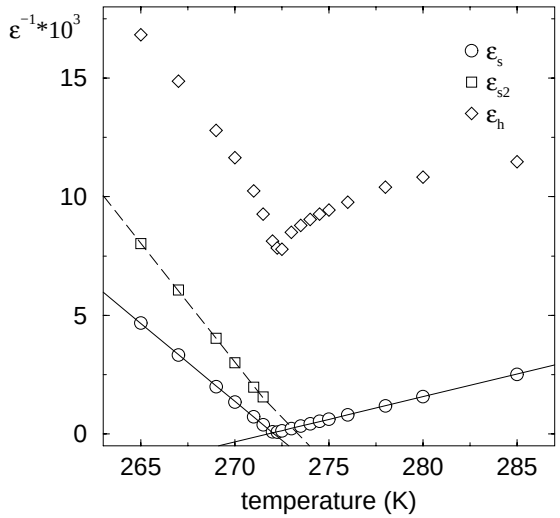

Fig. 2. Curie-Weiss plot of the low (ϵ_s, circles) and high-frequency (ϵ_h, diamonds) limit values of the permittivity. Squares refer to the contribution of the critical relaxation process within the ferroelectric region (ϵ_{s2}).

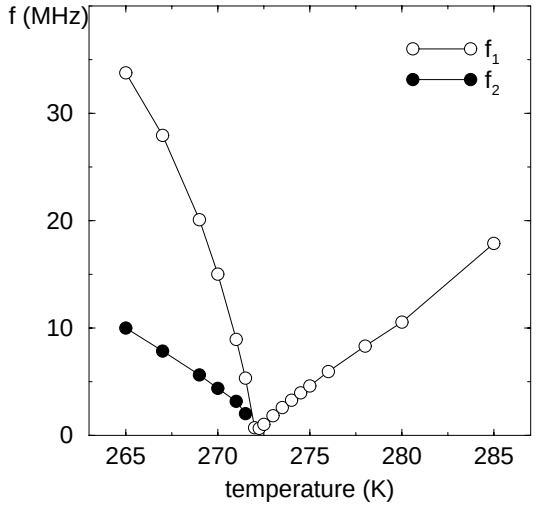

Fig. 3. Temperature dependence of the relaxation frequencies of K_2ZnI_4 around T_c. Open circles: critical relaxation process, filled circles: domain wall relaxation. The lines are guides to the eye.

The characteristic frequency f_1 of the Debye like relaxator reaches a minimum at T_c (Fig. 3). Within the paraelectric regime its behaviour follows that of ϵ_s^{-1}. Below T_c, the temperature dependence of f_1 differs somewhat from a classical Curie-Weiss law. Nevertheless, this dispersion process with its critical slowing-down behaviour near T_c is part of the transition mechanism.

The second relaxator, which was detected only in the ferroelectric regime, is of Cole-Cole type. Its distribution of relaxation times becomes distinctly broader with decreasing temperature, leading to a distribution parameter of $h_2 = 0.28$ at 265 K. This low frequency dispersion exhibits the characteristic features of ferroelectric domain wall motions.

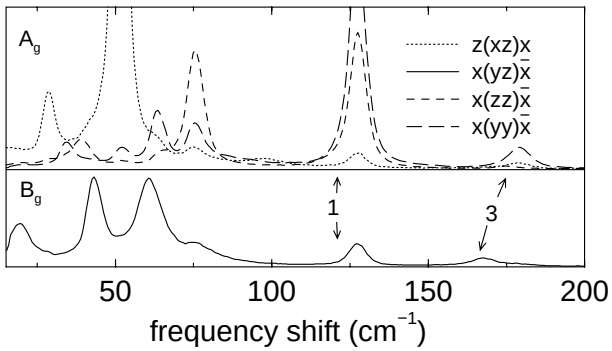

Fig. 4. Raman spectra of K_2ZnI_4 at ambient temperature. Above: $x(yy)\bar{x}$, $x(zz)\bar{x}$ and $z(xz)x$ geometry, according to A_g modes, below $x(yz)\bar{x}$, representing B_g modes. Intensity in arbitrary units. Some spectra have been scaled for presentation purposes.

4 Raman spectroscopic investigations

Polarized Raman spectra were recorded by means of a Jobin-Yvon triple spectrometer (T64000) with a photon counting system and a CCD multichannel detector. A coherent Ar^+ ion laser ($\lambda = 514.32$ nm) served as excitation source. We investigated thin (100)-plates (typical dimensions $3 \times 3 \times 0.5$ mm^3) in several backscattering geometries ($x(yy)\bar{x}$, $x(zy)\bar{x}$ and $x(zz)\bar{x}$) using a microprobe equipment with a temperature-adjustable microscope stage which is cooled by liquid nitrogen. Furthermore, we took Raman spectra in a $z(xz)x$ scattering geometry on an oriented single crystal ($10 \times 10 \times 10$ mm^3). A closed-cycle helium cryostat was employed to cool this sample. All investigated crystals were enclosed in vacuum tight cuvettes, filled with dry helium gas and silicon oil. In order to exclude partially hydrated crystals from the investigation, all samples were tested for internal H_2O-vibrations in a frequency range between 3000 and 3800 cm^{-1}.

A survey of Raman spectra of all observed scattering geometries at ambient temperature is given in Figure 4. The spectra were recorded with the CCD camera at a resolution $\Delta\tilde{\nu}$ of better than 3 cm^{-1}. All observed phonon frequencies are below 200 cm^{-1}. There is a distinct gap between external lattice modes with frequencies less than 100 cm^{-1} and some peaks at 125 cm^{-1} and in the range between 175 and 180 cm^{-1}. The latter ones, marked as 1 and 3 in Figure 4, correspond to the internal Zn-I stretching modes ν_1 and ν_3 of the free ZnI_4^{2-}-complex, whose characteristic frequencies were determined by Delwaulle [12] as 120 cm^{-1} and 170 cm^{-1}, respectively. The two remaining I-Zn-I bending modes of the tetrahedron with $\nu_2 = 44$ cm^{-1} and $\nu_4 = 62$ cm^{-1} lie within the bulk of lattice modes and could not be identified.

Raman measurements exemplified by Figure 4 have been performed in a temperature range between 220 and 310 K. Since our attention was mainly directed to the temperature dependence of external lattice modes, additional high resolution single channel spectra ($\Delta\tilde{\nu} < 1$ cm^{-1}) of all geometries except $x(zz)\bar{x}$ were recorded by means

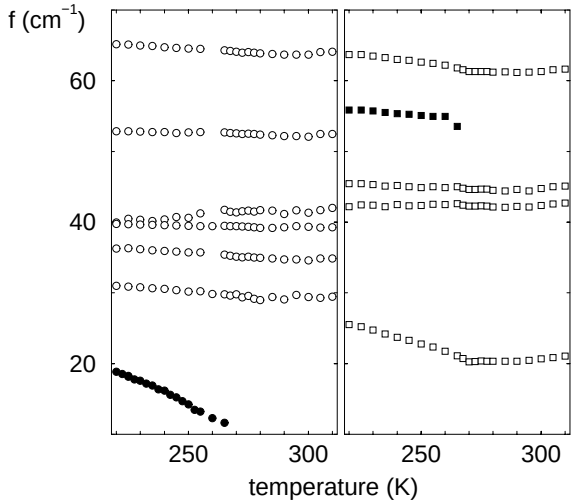

Fig. 5. Temperature dependence of the external lattice modes. Left side: A_g and A geometry, right side B_g and B geometry.

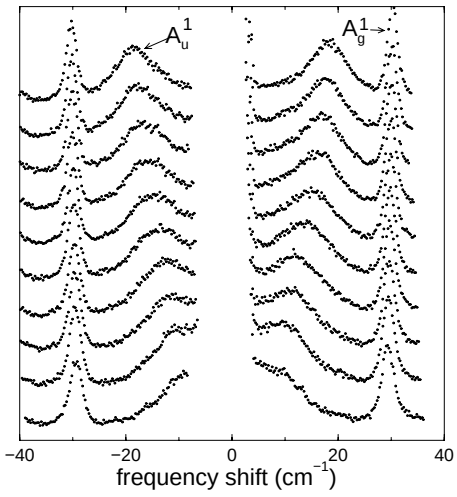

Fig. 6. The soft phonon A_u^1 and the mode A_g^1, recorded in the $z(xz)x$ scattering geometry. Bottom: spectrum at 260 K. The upper spectra correspond to temperatures successively lowered in steps of 5 K.

of the photomultiplier. The spectra were evaluated up to 70 cm^{-1} by fitting them to the response function of independent damped harmonic oscillators. The temperature dependence of the resulting eigenfrequencies are displayed in Figure 5. The right and left part of the figure refer to modes of the irreducible representations A and B of the symmetry class 2, respectively. Open symbols represent modes which are visible above as well as below T_c and, therefore, belong to the even symmetry species A_g and B_g of the paraelectric symmetry class $2/m$. Modes which transform according to the corresponding odd species A_u and B_u are not Raman active above T_c. They are displayed as full symbols in the ferroelectric regime.

Most of the mode frequencies increase slightly with decreasing temperature and exhibit no specific effects at T_c within the experimental accuracy. Preliminary analyses of the frequency range above 70 cm^{-1} show that this also holds true for the internal modes. The lowest mode of A_g symmetry, henceforth abbreviated as A_g^1, is a typical example of such phonons (Figs. 6, 7). However, the two modes with the lowest observed frequencies differ significantly from this behaviour and can be characterized as softening. The one with the lowest frequency (A_u^1) can be detected only below T_c and in $z(xz)x$ scattering geometry and is therefore attributed to the symmetry species A_u above T_c (Fig. 6). Its frequency decreases distinctly when approaching the transition temperature. Owing to Rayleigh scattering, the numerical determination of the characteristic frequency was only possible for temperatures below 265 K. We estimated $\nu_{A_u^1}(T_c)$ by a linear regression of the squared frequency to about 9 cm^{-1} (see Fig. 7). Above 260 K the phonon linewidth becomes larger than the eigenfrequency, *i.e.* the mode is overdamped in the vincinity of T_c.

The second softening phonon (B_g^1) belongs to the symmetry species B_g of the paraelectric phase. Its frequency decreases very slightly with decreasing temperature within the paraelectric regime but increases strongly below T_c.

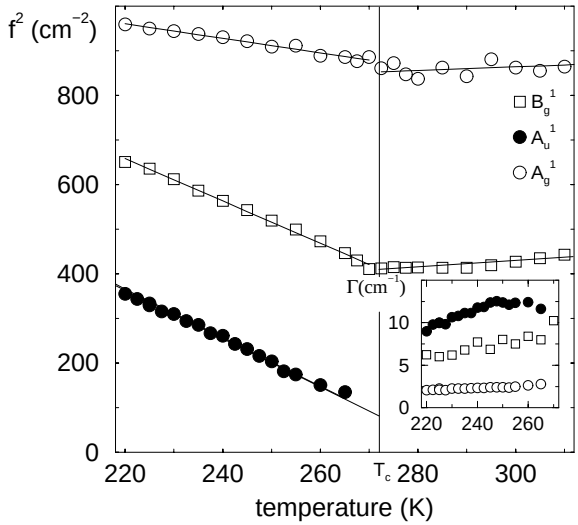

Fig. 7. Temperature dependence of the squared frequencies of the soft-mode A_u^1, the softening mode B_g^1 as well as of the lowest mode of A_g symmetry (A_g^1). Inset: the corresponding damping factors below T_c.

The characteristic linewidth is large compared with other phonons, except the mode A_u^1. However, a quantitative temperature dependence cannot be derived at this stage. This is a consequence of the $x(yz)\bar{x}$-backscattering geometry which we used for the detection of B/B_g phonons. The Rayleigh scattering in these spectra is large compared with a 90° scattering geometry which makes it impossible to obtain the linewidth for this mode with a higher accuracy.

5 Discussion

The experimental results in Sections 3 and 4 confirm the assumption that K_2ZnI_4 undergoes a proper ferroelectric transition, accompanied by a change in symmetry from $P2_1/m$ to $P2_1$. The transition is continuous within our experimental accuracy. We did not measure a physical property which may be considered the order parameter. However, the linear temperature dependence of ϵ_s^{-1} (Fig. 2) and of the squared frequency of the soft-mode A_u^1 (Fig. 7) indicates a classical mean field behaviour. The ratio of slopes of the reciprocal quasistatic permittivity without the contribution of domains was determined to about -5.25. A value of -6.0 results from a similar evaluation of f_1. These values differ distinctly from the theoretical prediction of -2 for second order phase transitions and isothermal and free conditions [13]. Interpreting these results, one has to take into account that the experimental values refer to the clamped crystal and adiabatic conditions. Different boundary conditions may cause deviations in the slope ratios [11]. However, it is noteworthy that the experimental values for K_2ZnI_4 are in good agreement with those of K_2ZnBr_4. This compound is assumed to undergo its ferroelectric phase transition at ambient pressure near to a tricritical point [7].

The dielectric and Raman spectroscopic measurements provide a detailed picture of the dynamics at the ferroelectric phase transition in K_2ZnI_4. The main conclusion from experimental results is that there are clearly two different processes involved in the transition mechanism. The process with the slower dynamics is a relaxational one and contributes more than 99% of the Curie-Weiss part of the permittivity at T_c. Its dispersion displays a critical slowing down and exhibits all features of a classical order-disorder process. The value of 5200 K for C is also typical for a ferroelectric of the order-disorder type [14]. We ascribe this dispersion to the ordering process of the disordered ZnI_4^{2-}-tetrahedra, in accordance with the partially disordered structure proposed by Kasano *et al.* [8].

Although the order-disorder component determines almost completely the dielectric properties of K_2ZnI_4, the transition mechanism also includes another important component. We mentioned in Section 3 that the temperature dependence of ϵ_h indicates another dispersion process at frequencies significantly above 1 GHz. This assumption is also supported by the atomic displacements in the ferroelectric phase (Fig. 8, left picture). The potassium ions are appreciably shifted almost parallel to the monoclinic axis, although they do not display disorder above T_c. Therefore, the postulated second part of the transition mechanism, which is responsible for these effects, should be displacive and transform according to representation A_u of the paraelectric phase. Indeed, a soft phonon of this symmetry has been detected in the Raman scattering experiments. A comparison of the relaxation frequency of the dielectric dispersion with the Raman shift of the A_u^1-soft-mode at 265 K (1.2×10^{-3} cm^{-1} and 11.6 cm^{-1}, respectively) shows that the latter one is connected with a further part of the transition mechanism. The A_u^1-mode is well described by a damped oscillator and it is not compatible with a relaxational effect, confirming the above predictions.

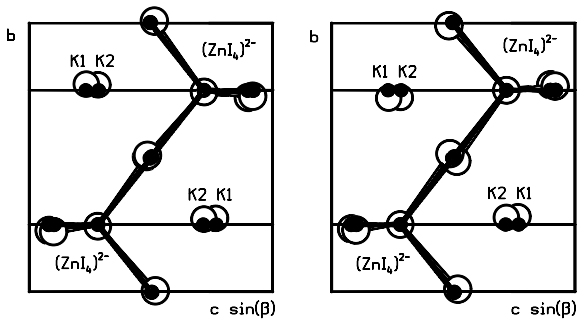

Fig. 8. Projections of the unit cell of K_2ZnI_4 along the a-axis. Straight lines at $b = 0.25$ and 0.75 refer to mirror planes. Filled symbols: time averaged structure at 296 K. Left picture: a comparison with the ferroelectric structure at 235 K (open symbols). Right picture: a proposal for the eigenvector of the softening phonon B_g^1 (see text). Structural data according to Kasano *et al.* [8].

Another interesting fact is the occurrence of a second softening mode of B_g-symmetry, whose temperature dependence of its frequency and linewidth resembles strongly those of the soft mode A_u^1. Although a linear coupling between a B_g phonon and the order parameter is forbidden by symmetry and the mode does not contribute to the ferroelectric displacement pattern, it turns out to be highly influenced by the phase transition. The existence of several softening modes of different symmetry is often observed in systems in which the symmetry is realized by a time averaged structure [15]. Therefore, the behaviour of the mode B_g^1 may be considered as a further indication of disorder in K_2ZnI_4.

In order to understand the coupling of the modes A_u^1 and B_g^1 to the disorder of the ZnI_4^{2-} complex, one has to consider the eigenvectors of these phonons. Crossing the phase transition, the two tetrahedra of a unit cell were tilted *in phase* around the a-axis, breaking the inversion and mirror symmetry (Fig. 8, left picture). Together with the shift of the potassium ions, this displacement represents at least in part the eigenvector of the soft phonon A_u^1. Considering a single ZnI_4^{2-} complex, the normal coordinate of A_u^1 almost matches the movement of the tetrahedron during a jump between its two positions. This explains the correlation between the dynamics of the relaxation process and the A_u soft mode. A comparison of the symmetry coordinates of B_g modes with those of A_u shows that they differ only in the phase shift between both formula units. Furthermore, the eigenfrequency of the phonon B_g^1 is small in comparison with the frequencies of the internal vibrations of the ZnI_4^{2-} complex [12]. This indicates that the tetrahedra are also acting as rigid bodies in this normal vibration. We assume, therefore, that the movement of the ZnI_4^{2-} tetrahedra of the phonon B_g^1

is very similar to the normal coordinate of A_u^1, except that the tetrahedra are tilted *out of phase* (Fig. 8, right part). This could explain why the mode B_g^1 is also strongly influenced by the positional disorder, since the movement of a single tetrahedron would be almost identical for both the A_u and B_g softening modes. The anomalous linewidths of both phonons can be ascribed to the anharmonic effects owing to the positional disorder, which turns out to be significant especially for these two modes due to their normal coordinates as well as to their weak harmonic restoring forces.

In conclusion the ferroelectric phase transition in K_2ZnI_4 can be classified as partially order-disorder and partially displacive. The dynamic features are in good agreement with structural investigations. The results resemble very much those found in K_2ZnBr_4, so that the transition mechanisms in both compounds are of a similar type. Now we are going to perform lattice dynamical calculations to verify our predictions concerning the displacement patterns of the low frequency lattice modes in this interesting new ferroelectric model system.

We would like to thank Mrs. K. Kretsch for technical assistance during the delicate sample preparations.

References

1. E. Philippot, M. Ribes, M. Maurin, Rev. Chim. Miner. **8**, 99 (1971), *in French*.
2. K. Gesi, J. Phys. Soc. Jpn **54**, 3694 (1985).
3. J. Fábry, Phase Trans. **53**, 61 (1995).
4. F. Shimizu, S. Sawada, M. Takashige, J. Phys. Soc. Jpn **65**, 870 (1996).
5. H. Kasano, M. Takesada, H. Mashiyama, J. Phys. Soc. Jpn **61**, 1580 (1992).
6. J. Fábry, T. Breczewski, F.J. Zúñiga, A.R. Arnaiz, Acta Cryst. C **49**, 946 (1993).
7. M. Jochum, H.-G. Unruh, H. Bärnighausen, J. Phys-Cond. **6**, 5751 (1994).
8. H. Kasano, M. Kojima, T. Shouji, H. Mashiyama, Ferroelectrics **169**, 149 (1995).
9. T. Britz, H.-G. Unruh, Ferroelectrics **185**, 151 (1996).
10. F. Shimizu, T. Anzai, H. Sekiguchi, M. Takashige, S. Sawada, J. Phys. Soc. Jpn **63**, 437 (1994).
11. G. Luther, Phys. Stat. Sol. A **20**, 227 (1973).
12. M.L. Delwaulle, Compt. Rend. **240**, 2132 (1955).
13. R. Blinc, B. Žekš, *Soft Modes in Ferroelectrics and Antiferroelectrics* (North Holland, Amsterdam, 1974).
14. T. Mitsui, I. Tatsuzaki, E. Nakamura, *An Introduction to the Physics of Ferroelectrics* (Gordon and Breach, New York, 1976).
15. H.-G. Unruh, Ferroelectrics **183**, 1 (1996).